Available online at www.sciencedirect.com
ScienceDirect
Tetrahedron 63 (2007) 10630–10636
Tetrahedron

# Metabolism of α-ketol derivative of linolenic acid (KODA), a flowering-related compound, in *Pharbitis nil*

Kenji Kai,[a] Fumihiko Yano,[b] Fumiya Suzuki,[b] Hideo Kitagawa,[b] Masayuki Suzuki,[b] Mineyuki Yokoyama[c] and Naoharu Watanabe[a,*]

[a]*Graduate School of Science and Technology, Shizuoka University, 836 Ohya, Suruga-ku, Shizuoka 422-8529, Japan*
[b]*Department of Applied Biological Chemistry, Faculty of Agriculture, Shizuoka University, 836 Ohya, Suruga-ku, Shizuoka 422-8529, Japan*
[c]*Material Science Research Center, Shiseido Co. Ltd, Tsuzuki-ku, Yokohama 224-8558, Japan*

Received 15 June 2007; revised 3 August 2007; accepted 3 August 2007
Available online 8 August 2007

**Abstract**—α-Ketol of octadecadienoic acid (KODA, **1**) has been suggested to play a role in the photoperiod-regulated flowering in *Pharbitis nil*. The level of **1** in cotyledons is temporarily controlled during short-day conditions. The biosynthesis of **1** is well studied in plants; however, its in vivo conversion is less understood. We have investigated this issue by studying the metabolism of exogenously-applied [U-$^{13}$C]-**1**, [1-$^{14}$C]-**1**, and non-labeled **1** in *P. nil* seedlings by the spectroscopic methods and identified six major metabolites (**4**–**9**). We have also found that the enantiomers of **1** are differentially metabolized in *P. nil* seedlings.


## 1. Introduction

Recent molecular-genetic approach in several species of plants, mainly *Arabidopsis thaliana*, allowed the discovery of several genes that control flowering times.[1,2] To date, it is generally accepted that *FT* and/or its translation product are the most promising candidate for florigen.[3–7] However, in *Arabidopsis*, *Lolium temulentum*, and *Pharbitis nil*, gibberellins were also shown to be active in the different regulation pathways from the *FT*/FT mediated systems of the flower initiation.[8–11] Therefore, it is plausible that unknown molecules play the regulatory roles in the floral initiation of plants. Studies of such components should be important for deeper understanding of the flowering of plants.

(12*Z*,15*Z*)-9-Hydroxy-10-oxo-12,15-octadecadienoic acid (KODA, **1**) (Fig. 1), an oxylipin, was isolated as a stress-releasing compound from *Lemna paucicostata*.[12] The reaction products of **1** with norepinephrine (NE) show strong flower-inducing activity toward the seedlings. Investigations have revealed that 9*R*-11-{(2*S*,8*S*,10*S*,11*R*)-2,8-dihydroxy-7-oxo-11-[(*Z*)-2-phenyl]-9-oxa-4-azatricyclo[6.3.1.0$^{1,5}$]dodec-5-en-10-yl}-9-hydroxy-10-oxoundecanoic acid (FN1, **2**) and its C-9 epimer (FN2, **3**) were the major components in

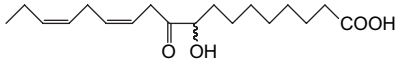


**1**

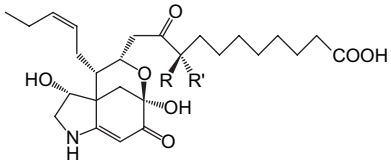


**2**: R = OH, R′ = H
**3**: R = H, R′ = OH

**Fig. 1**. Structures of compounds **1**, **2**, and **3**.

the reaction mixture, and that the former was active in flower induction whereas the latter was inactive.[13] These results from *L. paucicostata* have prompted us to investigate possible involvement of **1** in the flowering of other plant species.

*P. nil* (cv. Violet) widely used as a traditional plant in flowering studies is classified as a short-day plant that develops flower buds when cotyledons of four- to five-day-old seedlings are exposed to a single 16-h dark condition.[14] We have observed a close relationship between **1** and photoperiod-regulated flowering in *P. nil*.[15] The endogenous level of **1** in cotyledons of *P. nil* seedlings sharply increased at the end of flower-inducing dark conditions and dropped

*Keywords*: *Pharbitis nil*; Flowering; Floral induction; α-Ketol; Fatty acid; Metabolism; Structure elucidation.
* Corresponding author. Tel./fax: +81 54 238 4870; e-mail: acnwata@agr.shizuoka.ac.jp

0040–4020/$ - see front matter © 2007 Elsevier Ltd. All rights reserved.
doi:10.1016/j.tet.2007.08.012

rapidly to the basal level after the seedlings were exposed to light. Flower bud formation was also correlated with the elevated level of **1** within 11 to 16 h following the start of inductive dark period. This transient accumulation of **1** in cotyledons was not observed when seedlings were grown under continuous light. This is of great importance because very little is known about chemical changes in plants during the exposure to flower-inductive photoperiod and points to a possible role that **1** plays in the flowering of *P. nil*, as well as *L. paucicostata*. Exogenously-applied **1** does not induce the flowering in *P. nil*; however, it promotes the formation of flower buds once the plants were exposed to the inductive dark period.[15] Thus, metabolite(s) of **1**, for example cycloadduct with NE as described above, are expected to be in truly active form *in planta*. In our previous study, we investigated the change in the contents of catecholamines, including NE, and their structurally-related compounds in *P. nil* during the exposure to an inductive dark period.[16] It was found that their contents in the cotyledons did not change significantly throughout the experiment. Thus, it seems likely that catecholamines and their derivatives in *P. nil* do not interact with **1** during short-day induced flowering. Therefore, knowledge of in vivo conversion of **1** is essential in understanding the interaction between **1** and flower induction.

Because little is known about the metabolism of ketol derivative of fatty acids, many aspects of metabolism of **1** in *P. nil* are proposed. We have, therefore, sought to address this issue by identifying the metabolic pathways of **1** under the different photoperiods that induce or do not induce flower formation in *P. nil*. Previous studies have indicated the importance of chirality at C-9 for flowering.[13,17] Therefore we have also studied the effect of chirality on the metabolism by feeding experiments with 9*R*-**1** and 9*S*-**1**.

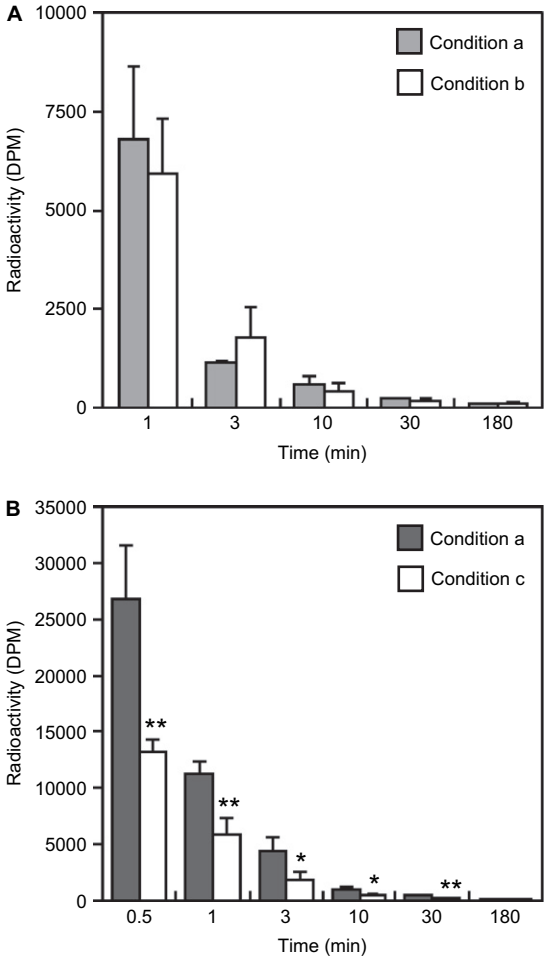


**Fig. 2**. Time-course studies on the in vivo conversion of [1-$^{14}$C]-**1** in *P. nil*. Comparisons of disappearance of [1-$^{14}$C]-**1** between conditions a and b (A)/ a and c (B) were described. The error bars indicate the standard deviations of three replicates. $^{**}P<0.01$ and $^{*}P<0.05$.

## 2. Results and discussion

### 2.1. Feeding study of [1-$^{14}$C]-1 in *P. nil*

Our previous experiment revealed that elevated levels (175–180 pmol/g tissue) of **1** in the 16-h dark-treated cotyledons of *P. nil* immediately reduced to normal (25–30 pmol/g tissue) after exposure to light.[15] Therefore, in order to explore the relationship between the metabolism of **1** and inductive photoperiod, [1-$^{14}$C]-**1** was administered to the cotyledons under three different conditions of dark/light periods: (a) five-day-old seedlings of *P. nil* were exposed to 16-h dark, and then the cotyledons were immersed in a solution of **1** under reduced pressure followed by incubating the seedlings under light for various times from 0.5 to 180 min; (b) same as 'a' except that the seedlings treated with **1** were incubated in continuous dark; (c) *P. nil* seedlings exposed to 16-h light were treated with **1** and subsequently kept under continuous light conditions. The amount of [1-$^{14}$C]-**1** incorporated into the cotyledons was evaluated by measuring the radioactivity in the residual solution to be ca. 300 pmol/g tissue, suggesting that the physiological amount of [1-$^{14}$C]-**1** was incorporated into the cotyledons. The radioactivity of **1** immediately disappeared in all experiments (Fig. 2). Significant differences in the metabolism of applied **1** were observed between conditions a and c, whereas conditions a and b did not show any significant differences. Exogenously-applied [1-$^{14}$C]-**1** was metabolized 2-times faster in condition a than in condition c. This suggests that a flowering-inductive dark period facilitates the metabolism of **1** and/or that continuous light suppresses it.

In these experiments, the high radioactivity was also observed in the fraction eluted at 10.0–10.5 min within 10 min after the treatment with [1-$^{14}$C]-**1** (Fig. 3A), suggesting that **1** was rapidly metabolized into the more polar compound. However, no radioactivity was observed in the extract of *P. nil* after additional 20 min, suggesting that β-oxidation occurred in these compounds and resulted in loss of radioactivities. Hence, [1-$^{14}$C]-**1** appeared to be an inappropriate tracer to examine metabolism of **1** in more detail.

### 2.2. Profiling analysis of the metabolites of 1 in *P. nil*

In order to study the dynamics, cold **1** was fed as in condition a to the seedlings of *P. nil*. Six major metabolites of **1** (**4**–**9**, Fig. 3B) could be detected in the treated sample, while these were not found in the control experiment. Among the metabolites, the retention time of **4** (10.1 min) was coincident

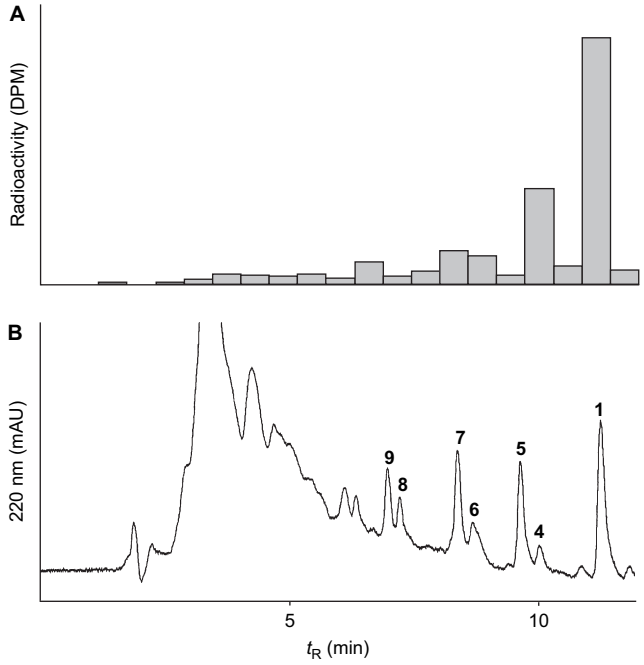


**Fig. 3**. HPLC profiles from *P. nil* seedlings fed [1-$^{14}$C]-**1** (A) and **1** (B). Five-day-old seedlings were immersed in the respective solutions, and incubated for 10 min under light (condition a). The retention times for metabolites **4**, **5**, **6**, **7**, **8**, and **9** are 10.1, 9.6, 8.7, 8.3, 7.1, and 6.8 min, respectively.

with that of the radioactive fraction (10.0–10.5 min) obtained upon feeding with a physiological level of [1-$^{14}$C]-**1** (Fig. 3A and B). Thus the same metabolism occurred in the both experiments, although the amount of **1** fed to the cotyledons was much higher than the physiological level. Metabolites **4** and **5** were detected first followed successively by **6**–**9**. Of the six metabolites, **8** and **9** were most likely to be end products, since other metabolites disappeared within first 60 min following the start of the administration of **1**. After 90 min, none of these metabolites could be detected and the resultant HPLC chromatogram was similar to that of control experiment. These results demonstrate that **1** is metabolized by the following route: **1**→(**4**, **5**)→(**6**, **7**)→(**8**, **9**). As mentioned above, **4** showed identical retention time with the metabolite that was derived from [1-$^{14}$C]-**1**. This indicated that **5**–**9** were β-oxidative products of **1** because relevant radioactivity could not be detected in any of these after 10 min as shown in Figure 3A.

### 2.3. Identification of metabolites 4–9

Compounds **4**–**9** were purified by preparative HPLC and each purified fraction was subjected to MS/MS analysis. Moreover, these metabolites were prepared by similar method but using [U-$^{13}$C]-**1** to acquire their $^{13}$C NMR and INADEQUATE spectral data based on the vicinal $^{13}$C–$^{13}$C couplings.

The negative ion mass spectrum of **4** gave ions at *m*/*z* 293 $[M-H-H_2O]^-$ and 275 $[M-H-2H_2O]^-$ suggesting the loss of two hydroxy groups from the deprotonated molecule $[M-H]^-$ at *m*/*z* 311 (Fig. 4). $^{13}$C NMR spectrum of **4** showed 18 signals with $^{13}$C–$^{13}$C couplings, of which a carbonyl carbon in **1** at C-10 position ($\delta_C$ 210.1 ppm) was reduced to hydroxymethine ($\delta_C$ 76.1 ppm) (Table 1). INADEQUATE spectrum confirmed the linkages from C-7 to C-18 (Fig. 5). These results gave the planar structure of **4** as (12*Z*,15*Z*)-9,10-dihydroxy-12,15-octadecadienoic acid generated from **1** via reduction of 10-carbonyl group. The MS/MS analysis of **5** showed fragment ions at *m*/*z* 263, 237, 219, and 183 from the deprotonated molecule $[M-H]^-$ at *m*/*z* 281 (Fig. 4). This fragmentation pattern was similar to that of **1**, except that the product ions were smaller by 28 mass units corresponding to ethylene fragment. Thus, it is likely that **5** was synthesized from **1** via β-oxidation. In line with this observation, the $^{13}$C NMR data of [U-$^{13}$C]-**5** showed 16 carbon signals, where the loss of two methylene carbons of **1** was observed (Table 1). INADEQUATE spectrum of [U-$^{13}$C]-**5** confirmed the respective bond connections of C-1 to C-8 and C-10 to C-16 carbons (Fig. 5). Thus, **5** was revealed to be (10*Z*,13*Z*)-7-hydroxy-8-oxo-10,13-hexadecadienoic acid, a β-oxidative product of **1**. Deprotonated molecules $[M-H]^-$, *m*/*z* 283, of **6** and **7** showed fragment ions at *m*/*z* 265, 247, 173, and 143 (Fig. 4) indicating these to be isomers. Based on the molecular weight and mass fragmentation pattern, **6** and **7** were predicted to be formed from either **4** via β-oxidation or **5** via reduction of carbonyl group. The $^{13}$C NMR spectra of [U-$^{13}$C]-**6** and [U-$^{13}$C]-**7** displayed characteristic carbon signals of carboxylic acid, two hydroxymethines, and diene among 16 carbon signals (Table 1). These fragments could be connected by the INADEQUATE experiments (Fig. 5). Metabolites **6** and **7** were confirmed as diastereomers of (10*Z*,13*Z*)-7,8-dihydroxy-10,13-hexadecadienoic acid. The observed fragment ions of **8** and **9** at *m*/*z* 237, 219, and 145 could be derived from deprotonated molecules $[M-H]^-$ at *m*/*z* 255 (Fig. 4) suggesting two cycles of β-oxidation and α-ketol reduction. By comparing the $^{13}$C NMR data of other metabolites, the carbon signals of [U-$^{13}$C]-**8** and [U-$^{13}$C]-**9** were assigned (Table 1) and structures of **8** and **9** were determined to be diastereomers of (8*Z*,11*Z*)-5,6-dihydroxy-8,11-tetradecadienoic acid.

On the basis of above discussions, the metabolic route of **1** in *P. nil* is shown in Figure 6. The pathways comprise of α-ketol reduction and β-oxidation cycle of straight-chain acid. The MS/MS analysis of the extract of *P. nil* also indicated some other metabolites, for example, possible β-oxidation product of **5**; however, these could not be characterized due to difficulties in purification. Thus, further β-oxidation of the metabolites of **1** is likely in plants. β-Oxidation enzymes specific for fatty acids of particular chain length are involved in the biosynthesis of oxylipin plant hormone jasmonate.[18] Further studies are needed to determine the involvement of specific enzymes to mediate the conversion of **1** to **4**–**9** via reduction and β-oxidation, and to determine the role of metabolism in controlling the activity of **1** in *P. nil*.

### 2.4. The metabolism of 9*R*-1 and 9*S*-1

It has been demonstrated that incubation of 9*R*-**1** with NE produces a flower-inducing factor known as **2**. On the other hand, compound **3**, C-9 epimer of **2**, derived from 9*S*-**1** did not show any flower-inducing activity.[13] In addition, Yokokawa et al. demonstrated that the activity of 9*R*-**1** was approximately 2-fold higher than that of (±)-**1** in *P. nil*.[17]

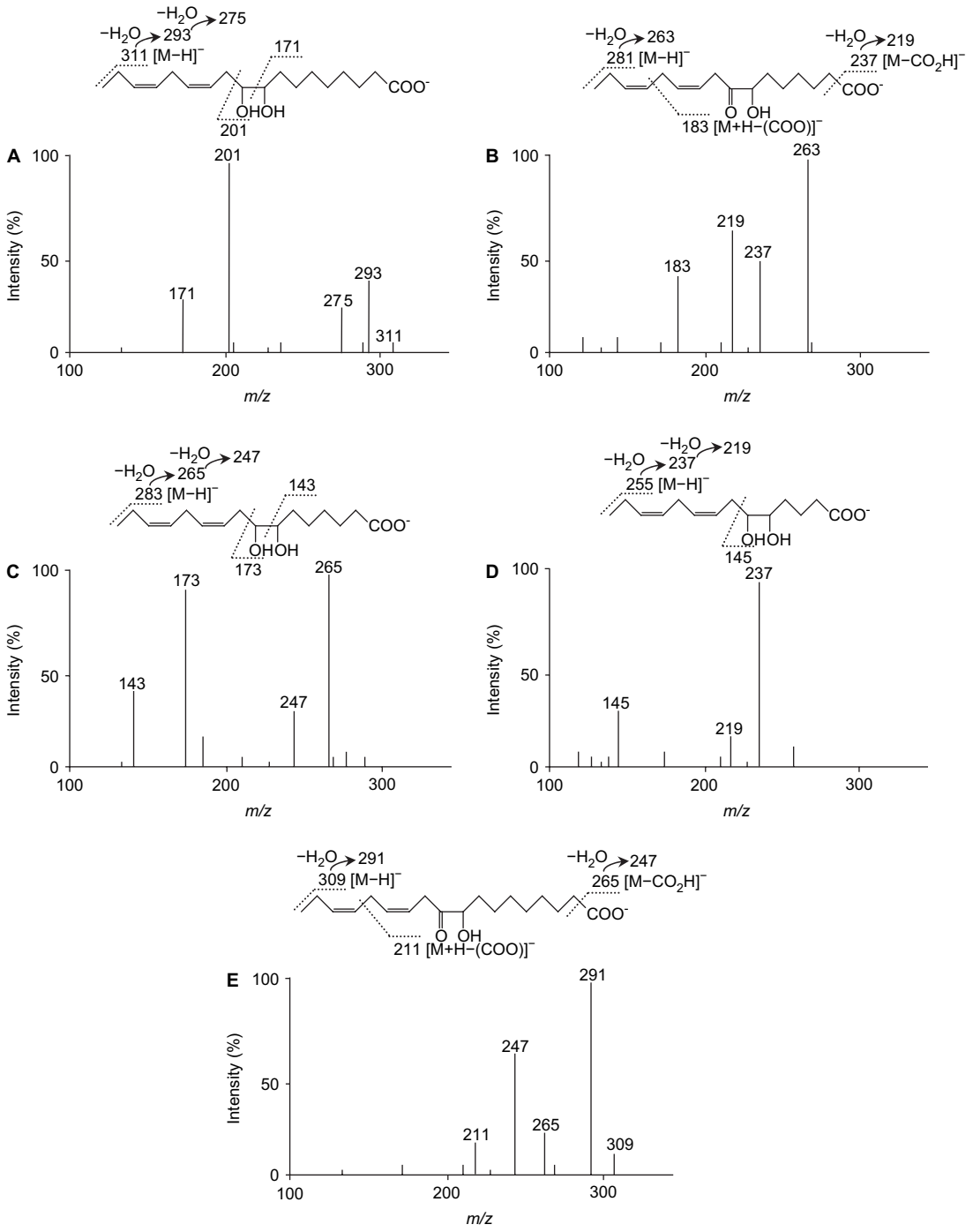


**Fig. 4**. Product-ion spectra of **4** (A), **5** (B), **6/7** (C), **8/9** (D), and **1** (E). They were monitored by negative electrospray ionization MS/MS for deprotonated molecule $[M-H]^-$. Proposed fragmentation patterns of respective metabolites and **1** are also shown.

Therefore, absolute configuration of **1** at C-9 is important for the flowering. This raised another important question, whether the metabolic pathways of 9*R*-**1** and 9*S*-**1** were same or different in the seedlings of *P. nil*. The preliminary experiment revealed that chirality of **1** at C-9 position was not changed during the extraction and purification steps. Hence, to examine the above document, feeding experiments were conducted and 9*R*-**1** and 9*S*-**1** were separately fed to the seedlings.

The metabolites of both 9*R*-**1** and 9*S*-**1** gave a single peak corresponding to 7*R*-**5** and 7*S*-**5** in both LC–MS (Fig. 7) and chiral HPLC analyses (see Section 4), indicating that β-oxidation did not cause epimerization of **1**. This is also supported by the general mechanism of β-oxidation.[18] Reduction of **1** to **4** was suggested to be enantio-selective at C-10 position, since isomers of **4** derived from 9*R*-**1** and 9*S*-**1** show different HPLC characteristics (dominant one detected at 10.6 and 10.9 min, respectively). The determination of absolute configuration of these metabolites is now in progress, which will support the enantio-selectivity in the reduction. The LC–MS profiles for further metabolites were confusing. Diols **6** and **7** derived from both 9*R*-**1** and 9*S*-**1** show the identical LC characteristics. This provides

**Table 1**. $^{13}C$ NMR spectral data for metabolites [U-$^{13}C$]-**4**–**9**

| No. | $\delta_C$ (ppm), multi., $J$ (Hz) | | | | | |
|---|---|---|---|---|---|---|
| | **4** | **5** | **6** | **7** | **8** | **9** |
| 1 | 179.4 (d, 55) | 178.7 (d, 55) | 180.7 (d, 53) | 180.3 (d, 52) | 180.6 (d, 55) | 182.3 (d, 54) |
| 2 | 36.2 (dd, 34, 55) | 35.7 (ddd, 3, 34, 55) | 37.6 (m) | 37.1 (dd, 33, 52) | 37.3 (m) | 38.8 (m) |
| 3 | 26.9 (t, 34) | 25.9 (t, 34) | 27.1 (t, 33) | 26.7 (t, 33) | 23.4 (t, 36) | 23.7 (t, 35) |
| 4 | 27.0 (m) | 30.1 (dt, 35, 3) | 30.7 (t, 33) | 30.5 (dd, 33, 35) | 33.9 (t, 36) | 33.5 (t, 35) |
| 5 | 30.5 (m) | 26.2 (t, 35) | 30.1 (t, 33) | 26.9 (t, 35) | 74.3 (dd, 36, 42) | 75.3 (dd, 35, 39) |
| 6 | 30.5 (m) | 34.4 (t, 35) | 34.0 (dd, 33, 35) | 33.5 (t, 35) | 75.2 (dd, 36, 42), | 76.1 (dd, 39, 43) |
| 7 | 30.5 (m) | 77.8 (m) | 74.5 (dd, 35, 40) | 75.4 (dd, 35, 41) | 32.0 (t, 42) | 31.6 (t, 43) |
| 8 | 33.6 (dd, 35, 36) | 213.0 (dd, 38, 42) | 75.2 (t, 40) | 76.1 (dd, 36, 41) | 127.3 (dd, 42, 69) | 127.6 (dd, 43, 69) |
| 9 | 74.5 (dd, 36, 41) | 37.6 (m) | 32.1 (t, 40) | 31.6 (t, 41) | 131.0 (dd, 41, 69) | 130.7 (dd, 42, 69) |
| 10 | 76.1 (dd, 40, 47) | 122.1 (dd, 43, 71) | 127.5 (dd, 40, 71) | 127.5 (dd, 41, 70) | 26.5 (t, 41) | 26.5 (t, 42) |
| 11 | 31.7 (t, 40) | 132.5 (dd, 42, 71) | 130.6 (dd, 41, 71) | 130.6 (dd, 42, 70) | 128.3 (dd, 41, 69) | 128.3 (dd, 42, 70) |
| 12 | 127.5 (dd, 40, 71) | 26.6 (t, 42) | 26.5 (t, 41) | 26.6 (t, 42) | 132.5 (dd, 42, 69) | 132.4 (dd, 41, 70) |
| 13 | 130.8 (dd, 42, 71) | 127.6 (dd, 42, 71) | 128.4 (dd, 41, 70) | 128.3 (dd, 42, 70) | 21.4 (dd, 34, 42) | 21.4 (dd, 34, 41) |
| 14 | 26.6 (t, 42) | 133.1 (dd, 42, 71) | 132.2 (dd, 41, 70) | 132.5 (dd, 42, 70) | 14.7 (d, 34) | 14.7 (d, 34) |
| 15 | 128.3 (ddd, 42, 70) | 21.5 (ddd, 4, 34, 42) | 21.5 (dd, 35, 41) | 21.5 (ddd, 4, 34, 42) | | |
| 16 | 132.7 (dd, 42, 70) | 14.6 (d, 34) | 14.7 (d, 35) | 14.6 (d, 34) | | |
| 17 | 21.5 (ddd, 4, 34, 42) | | | | | |
| 18 | 14.6 (d, 34) | | | | | |

Taken in $CD_3OD$ at 125 MHz.

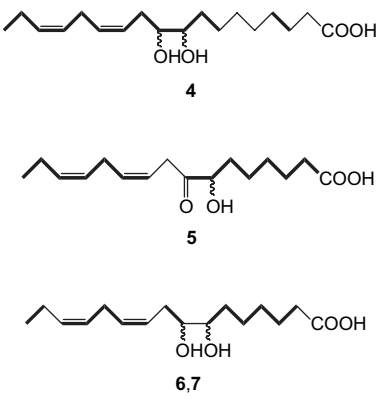


**Fig. 5**. Direct carbon correlations of **4**–**7** observed in INADEQUATE experiments. Bold line represents the observed correlations.

the suggestion that the enantio-selectivity of keto-reductase toward **5**, which has a shorter carbon chain than **1**, could be ambiguous. On the other hand, relevant differences were observed for metabolites **8** and **9** as shown in Figure 7. As yet, we have no convincing insight about this matter. These may give the reason for the difference in biological activity between 9*R*-**1** and 9*S*-**1**.

## 3. Conclusion

The present study demonstrated that exogenously-applied **1** is mainly metabolized via β-oxidation and reduction. The metabolism of **1** in *P. nil* is regulated in accordance with the flowering-inducing photoperiods. These studies have also demonstrated the importance of chirality of **1**. Further study is necessary to establish the physiological relevance of the observed metabolic pathway. The activities of these metabolites toward floral induction and its promotion need to be evaluated. At present, many genes related to the

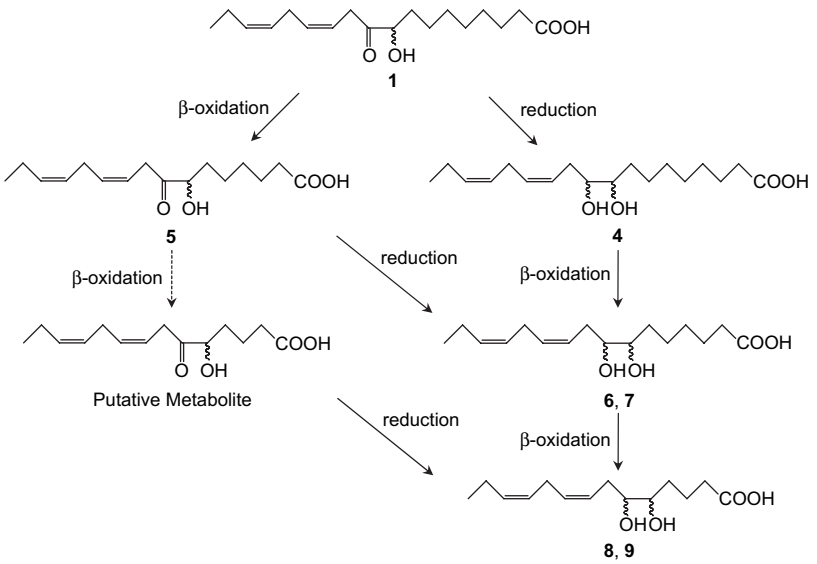


**Fig. 6**. Proposed metabolic pathway of **1** in *P. nil*.

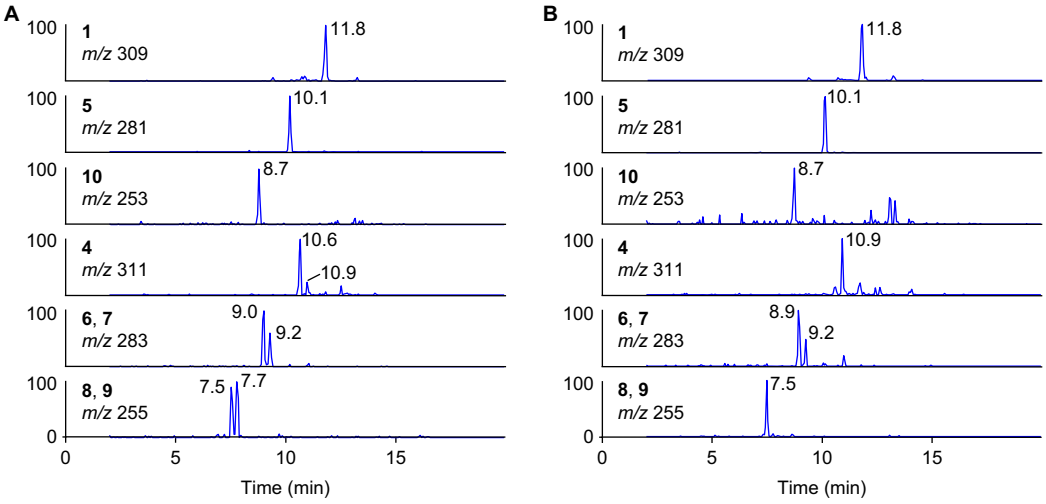


**Fig. 7**. LC–MS chromatograms of extracts of the seedlings to which 9*R*-**1** (A) and 9*S*-**1** (B) were applied. Each metabolites, **4**–**9**, were monitored by the selected ion monitoring (SIM) for deprotonated molecule $[M-H]^-$.

regulation of floral development have been elucidated mainly from *A. thaliana*.[1,2] In this respect, several of these genes were tentatively identified in *P. nil*,[19] suggesting that the similar mechanism was involved in the flowering. Examination of the interaction between **1** and metabolites **4**–**9** and the expression of such genes will give an important key to address the physiological role of **1** in flower formation.

## 4. Experimental

### 4.1. General procedures

$^{13}C$ NMR and INADEQUATE spectra were recorded on a JNM λ500A spectrometer (JEOL, Tokyo, Japan) using $CD_3OD$ as a solvent. LC–MS analysis was conducted with an LC-10VP system equipped with LCMS 2010A mass spectrometer (Shimadzu, Kyoto, Japan). LC–MS/MS experiments were carried out on a Survey HPLC system (Thermo Electron, MA, USA) equipped with LCQ Deca XP plus mass spectrometer (Thermo Electron). The HPLC analysis was performed with a JASCO (Tokyo, Japan) LC system. The solvent for HPLC was available from Kanto Chemical (Tokyo, Japan). A three-solvent system was used to generate the mobile phase for HPLC: solvent A, 0.05% (v/v) formic acid; solvent B, 0.05% (v/v) TFA; and solvent C, MeCN.

### 4.2. Plant material

*P. nil* (cv. Violet) was germinated as described previously.[20] Seeds of *P. nil* (Marudane, Kyoto, Japan) were immersed in concd $H_2SO_4$ for 20 min, and were subsequently washed in running water overnight. The seeds were placed on soil and incubated at 25 °C under continuous light (5000 lux). Five-day-old plants were transferred to Nakayama's liquid culture[21] and incubated at 25 °C under light (5000 lux) for 5–6 h to synchronize the growth of the seedlings.

### 4.3. Syntheses of 1, [1-$^{14}$C]-1, and [U-$^{13}$C]-1

Compounds **1**, [1-$^{14}$C]-**1**, and [U-$^{13}$C]-**1** were enzymatically synthesized from α-linolenic acid, [1-$^{14}$C]α-linolenic acid (909 nmol, 1.85 MBq, 55 mCi/mmol, Japan Radioisotope Association, Tokyo, Japan), and [U-$^{13}$C]α-linolenic acid ($^{13}C\%>98\%$, Spectral Gases Inc., NJ, USA), respectively.[12] HPLC analysis using a chiral column revealed that this method provided enantiomeric **1** (*R*:*S*=3:1). Optically-pure 9*R*-**1** and 9*S*-**1** were obtained by chiral HPLC separation [column, CHIRALPAK OD-RH 250 mm×20 mm (Daicel Chemical, Tokyo, Japan); flow rate, 10 mL/min; solvent, 40% (v/v) C/(A+C) for 30 min and thereafter gradient 40–43% (v/v) C/(A+C) within 30 min; temperature, 8 °C].

### 4.4. Feeding experiments and HPLC analyses

The cotyledons of *P. nil* were immersed in a solution of **1** ([1-$^{14}$C]-**1**, 125 ng/mL; **1** and [U-$^{13}$C]-**1**, 200 μg/mL; 9*R*/9*S*-**1**, 50 μg/mL) under reduced pressure (80 mmHg) for 1 min. After incubation for appropriate times, the seedlings were homogenized in liquid $N_2$ and extracted with EtOAc five times by sonication for 1 min. The extracts were combined and evaporated to dryness. The residue was dissolved in 20% (v/v) MeCN, and applied to a Supelclean ENVI-Chrom-P SPE (0.5 g) (SUPELCO, PA, USA). After washing with 20% (v/v) MeCN, **1** and its metabolites were eluted with 80% (v/v) MeCN from the column. The in vivo conversion of [1-$^{14}$C]-**1** was examined by the radioactivity of HPLC-purified fraction [HPLC conditions: column, CAPCELL PAK C18 UG 150 mm×4.6 mm; flow rate, 1.0 mL/min; solvent, 25–70% (v/v) C/(B+C) within 10 min and then 70–100% (v/v) C/(B+C) for 10 min; temperature, 40 °C]. Metabolic profiling of applied **1** was performed with following HPLC conditions: column, CAPCELL PAK C18 UG 150 mm×4.6 mm; flow rate, 1.0 mL/min; solvent, 25–75% (v/v) C/(B+C) within 10 min and thereafter 75–100% (v/v) C/(B+C) for 2 min; temperature, 40 °C; detection, 220 nm.

### 4.5. Isolation and structure determination of metabolites 4–9

*P. nil* seedlings (26 g fresh wt) previously immersed in a solution of **1** or [U-$^{13}$C]-**1** as described above and incubated for 10 min were extracted and partially-purified in accordance with feeding experiments. The former was subjected to

LC–MS/MS analysis operated in product-ion scan mode. HPLC conditions: column, CAPCELL PAK C18 UG 150 mm×2.0 mm; flow rate, 0.2 mL/min; solvent, 25–75% (v/v) C/(A+C) within 10 min and thereafter 75% (v/v) C/(A+C) for 2 min; temperature, 40 °C. MS conditions: spray temperature, 350 °C; CID energy, 10 V; collision gas, He.

For NMR analysis, the metabolites of [U-$^{13}$C]-**1** were purified by preparative HPLC under following conditions: column, CAPCELL PAK C18 UG 150 mm×4.6 mm; flow rate, 1.0 mL/min; solvent, 25–70% (v/v) C/(B+C) within 10 min and thereafter 70–100% (v/v) C/(B+C) for 2 min; temperature, 40 °C.

### 4.6. LC–MS analyses of the metabolites of 9*R*-1 and 9*S*-1

The cotyledons of *P. nil* were immersed in a solution of either 9*R*-**1** or 9*S*-**1** (25 μg/mL). The preparation of the samples was according to the method mentioned in Section 4.4. The LC–MS conditions were as follows, HPLC conditions: column, CAPCELL PAK C18 UG 150 mm×2.0 mm; flow rate, 0.2 mL/min; solvent, 25–75% (v/v) C/(A+C) within 10 min and thereafter 75% (v/v) C/(A+C) for 2 min; temperature, 30 °C. MS conditions: spray temperature, 350 °C. Chiral HPLC analysis of metabolite **5** was performed as follows, HPLC conditions: column, CHIRALPAK OD-RH 150 mm×4.6 mm; flow rate, 0.2 mL/min; solvent, 45% (v/v) C/(A+C); temperature, 8 °C. Compounds 9*R*-**1** and 9*S*-**1** gave the different retention times corresponding to the respective enantiomers of **5**, 22.5 and 21.0 min.

## Acknowledgements

A part of this work was supported by a grant-in-aid for N.W. from the Research and Development Program for New Bioindustry Initiatives.

## References and notes

1. Corbesier, L.; Coupland, G. *J. Exp. Bot.* **2006**, *57*, 3395–3403.
2. Imaizumi, T.; Kay, S. A. *Trends Plant Sci.* **2006**, *11*, 550–558.
3. Abe, M.; Kobayashi, Y.; Yamamoto, S.; Daimon, Y.; Yamaguchi, A.; Ikeda, Y.; Ichinoki, H.; Notaguchi, M.; Goto, K.; Araki, T. *Science* **2005**, *309*, 1052–1056.
4. Huang, T.; Bohlenius, H.; Eriksson, S.; Parcy, F.; Nilsson, O. *Science* **2005**, *309*, 1694–1696.
5. Lifschitz, E.; Eviatar, T.; Rozman, A.; Shalit, A.; Goldshmidt, A.; Amsellem, Z.; Alvarez, J. P.; Eshed, Y. *Proc. Natl. Acad. Sci. U.S.A.* **2006**, *103*, 6398–6403.
6. Corbesier, L.; Vincent, C.; Jang, S.; Fornara, F.; Fan, Q.; Searle, I.; Giakountis, A.; Farrona, S.; Gissot, L.; Turnbull, C.; Coupland, G. *Science* **2007**, *316*, 1030–1033.
7. Tamaki, S.; Matsuo, S.; Wong, H. L.; Yokoi, S.; Shimamoto, K. *Science* **2007**, *316*, 1033–1036.
8. Eriksson, S.; Bohlenius, H.; Moritz, T.; Nilsson, O. *Plant Cell* **2006**, *18*, 2172–2181.
9. King, R. W.; Evans, L. T.; Mander, L. N.; Moritz, T.; Pharis, R. P.; Twitchin, B. *Phytochemistry* **2003**, *62*, 77–82.
10. King, R. W.; Moritz, T.; Evans, L. T.; Martin, J.; Andersen, C. H.; Blundell, C.; Kardailsky, I.; Chandler, P. M. *Plant Physiol.* **2006**, *141*, 498–507.
11. King, R. W.; Pharis, R. P.; Mander, L. N. *Plant Physiol.* **1987**, *84*, 1126–1131.
12. Yokoyama, M.; Yamaguchi, S.; Inomata, S.; Komatsu, K.; Yoshida, S.; Iida, T.; Yokokawa, Y.; Yamaguchi, M.; Kaihara, S.; Takimoto, A. *Plant Cell Physiol.* **2000**, *41*, 110–113.
13. Yamaguchi, S.; Yokoyama, M.; Iida, T.; Okai, M.; Tanaka, O.; Takimoto, A. *Plant Cell Physiol.* **2001**, *42*, 1201–1209.
14. Imamura, S.; Takimoto, A. *Bot. Mag. Tokyo* **1955**, *68*, 235–241.
15. Suzuki, M.; Yamaguchi, S.; Iida, T.; Hashimoto, I.; Teranishi, H.; Mizoguchi, M.; Yano, F.; Todoroki, Y.; Watanabe, N.; Yokoyama, M. *Plant Cell Physiol.* **2003**, *44*, 35–43.
16. Suzuki, M.; Mizoguchi, M.; Yano, F.; Hara, U.; Yokoyama, M.; Watanabe, N. *Z. Naturforsch. C* **2003**, *58*, 220–224.
17. Yokokawa, Y.; Kobayashi, K.; Yokoyama, M.; Yamamura, S. *Chem. Lett.* **2003**, *32*, 844–845.
18. Howe, G. A. *Plant Hormones*; Davies, P. A., Ed.; Kluwer Academic: Dordrecht, 2004; pp 610–634.
19. Parfitt, D.; Herbert, R. J.; Rogers, H. J.; Francis, D. *J. Exp. Bot.* **2004**, *55*, 2169–2177.
20. Kaihara, S.; Kozaki, A.; Takimoto, A. *Plant Cell Physiol.* **1989**, *30*, 1023–1028.
21. Nakayama, S.; Hashimoto, T. *Plant Cell Physiol.* **1973**, *14*, 419–422.